Superfluid state in the periodic Anderson model with attractive interactions

Akihisa KOGA[1] * and Philipp WERNER[2]

[1] *Department of Physics, Tokyo Institute of Technology, Tokyo 152-8551, Japan*
[2] *Theoretische Physik, ETH Zurich, Zürich 8093, Switzerland*

We investigate the periodic Anderson model with attractive interactions by means of dynamical mean-field theory (DMFT). Using a continuous-time quantum Monte Carlo impurity solver, we study the competition between the superfluid state and the paramagnetic Kondo insulating state, and determine the phase diagram. At the chemical potential-induced phase transition from the Kondo insulating state to the superfluid state, a low-energy peak characteristic of the superfluid state appears inside the hybridization gap. We also address the effect of the confining potential in optical lattice systems by means of real-space DMFT calculations.

KEYWORDS: periodic Anderson model, superfluid, dynamical mean-field theory, optical lattice

1. Introduction

Ultracold atomic gases have attracted considerable interest[1–3] since the successful realization of Bose-Einstein condensation in a bosonic ^{87}Rb system.[4] One of the most active topics in this field is the study of fermionic optical lattice systems, which are formed by loading ultracold fermions into a periodic potential.[5–8] This setup provides a clean realization of a quantum lattice system, in which remarkable phenomena have been observed such as the Mott insulating state[9,10] and the BCS-BEC crossover in two component fermionic systems.[11–13] Due to the high controllability of the lattice structure and onsite interactions, ultracold fermionic systems in optical lattices can be regarded as quantum simulators of the Hubbard model, whose ground-state properties have been investigated by numerous theoretical and computational approaches. Recent papers have suggested the possible realization of optical lattice systems described by other theoretical models such as multi-component models[14–16] and the Kondo lattice model.[17–19] This stimulates further investigations on lattice models with strong correlations. Among them, the periodic Anderson model (PAM) describing conduction and localized bands is one of the most important models in condensed matter physics. It captures the essential physics of some heavy-electron systems realized in rare-earth compounds.[20] An

---

*E-mail address: koga@phys.titech.ac.jp

important point is that quantum critical behavior is expected in the PAM with both repulsive and attractive interactions, and the model may thus provide a stage to discuss a quantum phase transition in an optical lattice system. However, this type of instability, which may be important to predict the low-temperature properties of optical lattice systems, has not been discussed in the PAM with attractive interactions. Furthermore, the confining potential should play a crucial role in understanding the quantum critical behavior in optical lattice systems with attractive interactions. Therefore, it is important to systematically investigate the low temperature properties in this model with localized and itinerant bands.

In this paper, we study the PAM with attractive interactions by combining dynamical mean-field theory (DMFT)[21–24] with the continuous-time quantum Monte Carlo (CTQMC) approach.[25] First, we discuss how the superfluid state is realized on a uniform bipartite lattice and determine the phase diagram. By examining the dynamical properties in the superfluid state in detail, we demonstrate that low energy in-gap states are induced in the density of states. We also discuss the effect of the confining potential by means of the real-space DMFT and investigate how the Kondo insulating state spatially competes with the superfluid state.

The paper is organized as follows. In Sec. 2, we introduce the model Hamiltonian and explain the particle-hole transformation in the PAM. We briefly summarize our theoretical approach. We demonstrate how the superfluid state competes with the Kondo insulating state at low temperatures in Sec. 3. The effect of the confining potential is discussed in Sec. 4. A brief summary is given in the last section.

2. Model and Method

We consider the periodic Anderson model with conduction and localized bands, which is described by the following Hamiltonian,

$$H = H_0 + H_1, \tag{1}$$

$$H_0 = -t \sum_{\langle i,j \rangle \sigma} c_{i\sigma}^\dagger c_{j\sigma} + V \sum_{i\sigma} \left(c_{i\sigma}^\dagger f_{i\sigma} + f_{i\sigma}^\dagger c_{i\sigma} \right)$$

$$+ E_f \sum_{i\sigma} n_{i\sigma}^f - \sum_{ia\sigma} (\mu_a + h_a\sigma) \, n_{i\sigma}^a, \tag{2}$$

$$H_1 = -U \sum_i \left[n_{i\uparrow}^f n_{i\downarrow}^f - \frac{1}{2} \left(n_{i\uparrow}^f + n_{i\downarrow}^f \right) \right], \tag{3}$$

where $c_{i\sigma}(f_{i\sigma})$ annihilates a particle in the conduction (localized) band on the ith site with spin σ, and $n_{i\sigma}^a = a_{i\sigma}^\dagger a_{i\sigma}$　$(a = c$ and $f)$. t is the nearest-neighbor hopping matrix for the conduction band, V is the hybridization between the two bands, U is the attractive interaction,

and E_f is the energy level for the localized band. $\mu_c(\mu_f)$ and $h_c(h_f)$ are the chemical potential and the magnetic field for the conduction (localized) band. In the following, we refer to the conduction and localized bands as c and f bands, for simplicity.

First, we wish to note that the low-energy properties of the PAM with attractive interactions [eq. (1)] are closely related to those of the repulsive PAM. This can be understood by applying a particle-hole transformation to the model on the bipartite lattice. It is explicitly given by

$$\begin{cases} c_{i\sigma} \rightarrow \sigma \tilde{c}_{i\sigma}^{\dagger} \\ f_{i\sigma} \rightarrow -\sigma \tilde{f}_{i\sigma}^{\dagger} \end{cases} \quad i \in A, \tag{4}$$

$$\begin{cases} c_{j\sigma} \rightarrow -\sigma \tilde{c}_{j\sigma}^{\dagger} \\ f_{j\sigma} \rightarrow \sigma \tilde{f}_{j\sigma}^{\dagger} \end{cases} \quad j \in B, \tag{5}$$

where A and B are sublattice indices, and $\tilde{c}_{i\sigma}$ ($\tilde{f}_{i\sigma}$) annihilates a particle in the c (f) band on the ith site with spin σ. We then obtain the PAM with repulsive interactions $\tilde{U}(=-U)$, where the energy level for the f band, chemical potentials and magnetic fields are transformed as $\tilde{E}_f = 0$, $\tilde{\mu}_f = h_f$, $\tilde{\mu}_c = h_c$, $\tilde{h}_f = E_f - \mu_f$, and $\tilde{h}_c = \mu_c$, respectively. In particular, the low temperature properties of both models are equivalent at half filling ($E_f = 0, \mu_a = 0, h_a = 0$), which is similar to the case of the Hubbard model.[26]

The low-temperature properties of the PAM with repulsive interactions, which have been discussed in the context of f electron systems,[20] may be helpful to understand those of our attractive model. In the repulsive PAM, the hybridization between the c and f bands favors the formation of a local Kondo singlet state. Therefore, a large hybridization stabilizes the Kondo insulating state at half filling and the heavy metallic state away from half filing.[27, 28] On the other hand, the Coulomb repulsion favors magnetic correlations between sites, which tends to induce an antiferromagnetically ordered state.[29–33] Therefore, in the half-filled PAM on a bipartite lattice, a quantum phase transition occurs between the Kondo insulating state and the antiferromagnetically ordered state in two and higher dimensions. Note that this competition is controlled by not only the interaction strength but also the magnetic field. If a magnetic field is applied, the spin gap in the Kondo insulating state decreases and finally vanishes. At this point, a field-induced magnetic phase transition occurs, where a spontaneous staggered magnetization appears in the plane perpendicular to the applied field.[34–36]

In the PAM with attractive interactions, a similar competition is expected at low temperatures. The corresponding ordered phase should be characterized by a pair potential Δ,

which is given by

$$\Delta_a = \frac{1}{N} \sum_i \langle a_{i\uparrow} a_{i\downarrow} \rangle, \tag{6}$$

where $a = c, f$, and N is the total number of sites. This quantity corresponds to the staggered magnetization in the x direction $m_x^a = \frac{1}{N} \sum_i (-1)^i \langle \tilde{a}_{i\uparrow}^\dagger \tilde{a}_{i\downarrow} + \tilde{a}_{i\downarrow}^\dagger \tilde{a}_{i\uparrow} \rangle$ in the PAM with repulsive interactions. By contrast, it is known that the Kondo insulating state has no order parameter since it is adiabatically connected to the paramagnetic state at high temperatures. This implies that it is also realized in the PAM with attractive interactions.

To discuss how the superfluid state competes with the Kondo insulating state, we make use of DMFT. Since local particle correlations can be taken into account precisely, this method is formally exact in the limit of infinite dimensions, and has successfully been applied to strongly correlated systems. In DMFT, the lattice Green's function is obtained via a self-consistency condition imposed on the impurity problem. The non-interacting Green's function for the lattice model is given as,

$$\hat{G}_0^{-1}(k, i\omega_n) = \begin{pmatrix} \xi_c \sigma_0 + (\mu_c - \epsilon_k)\sigma_z & -V\sigma_z \\ -V\sigma_z & \xi_f \sigma_0 + (\mu_f - E_f)\sigma_z \end{pmatrix} \tag{7}$$

where $\xi_a = i\omega_n + h_a$ $(a = c, f)$, ϵ_k is the dispersion relation of the c band, σ_z is the z component of the Pauli matrix, σ_0 is the identity matrix, $\omega_n = (2n+1)\pi T$ is the Matsubara frequency, and T is the temperature. Here, the Green's function is represented in the Nambu formalism to describe the superfluid state. The lattice Green's function is then given in terms of the site diagonal self-energy $\hat{\Sigma}(i\omega_n)$ as,

$$\hat{G}(i\omega_n) = \begin{pmatrix} G_c(i\omega_n) & G_{cf}(i\omega_n) \\ G_{fc}(i\omega_n) & G_f(i\omega_n) \end{pmatrix} \tag{8}$$

$$= \int dk \left[\hat{G}_0^{-1}(k, i\omega_n) - \hat{\Sigma}(i\omega_n) \right]^{-1},$$

$$\hat{\Sigma}(i\omega_n) = \begin{pmatrix} 0 & 0 \\ 0 & \Sigma_f(i\omega_n) \end{pmatrix}. \tag{9}$$

The self-energy for the f band Σ_f is given as,

$$\Sigma_f(i\omega_n) = \begin{pmatrix} \Sigma_{f\uparrow}(i\omega_n) & S_f(i\omega_n) \\ S_f(i\omega_n) & -\Sigma_{f\downarrow}^*(i\omega_n) \end{pmatrix}, \tag{10}$$

where $\Sigma_{f\sigma}(i\omega_n)$ $[S_f(i\omega_n)]$ is the normal (anomalous) part of the self-energy for the f band. In DMFT, the self-consistency condition is given by

$$G_f(i\omega_n) = G_{imp}(i\omega_n), \tag{11}$$

where G_{imp} is the Green's function of the effective impurity model. The effective medium for each site is given by

$$\mathcal{G}^{-1}\left(i\omega_n\right) = \left[G_f\left(i\omega_n\right)\right]^{-1} + \Sigma\left(i\omega_n\right). \tag{12}$$

In the PAM with attractive interactions, a competition between the Kondo insulating state and the superfluid state is expected. Therefore, it is necessary that the impurity solver is capable of treating different energy scales accurately. The exact diagonalization method[37] is efficient to discuss ground state properties, but it is difficult to quantitatively discuss the critical behavior and dynamical properties at finite temperatures. The numerical renormalization group method[38,39] is one of the most powerful methods to describe the low energy states, but may not be appropriate for investigating the higher energy region. In this paper, we use the recently developed CTQMC method. In this approach, a Monte Carlo sampling of certain collections of diagrams is performed in continuous time, and thereby the Trotter error, which originates from the Suzuki-Trotter decomposition, is avoided. The CTQMC method comes in two flavors, a weak-coupling[25] and strong-coupling[40] formalism, and is applicable to general classes of models such as the Hubbard model,[41–46] the periodic Anderson model,[47] the Kondo lattice model,[48] and the Holstein-Hubbard model.[49] Here, we use the continuous-time auxiliary field version of the weak-coupling CTQMC method[50] extended to the Nambu formalism, which allows us to directly access the superfluid state at low temperatures.[45] In our CTQMC simulations, we measure normal and anomalous Green's functions on a grid of a thousand points. To discuss static and dynamical properties in the system quantitatively, the number of CTQMC samplings in each DMFT iteration is changed, depending on the temperature, the chemical potential, and the magnitude of the hybridization: *e.g.* we have performed eighty million (five billion) samplings for the half-filled system with $U = 1$, $V = 0.40$, and $T = 0.02$ ($U = 1$, $V = 0.18$ and $T = 0.01$). In the following, we set $\mu = \mu_c = \mu_f$ and $h = h_c = h_f = 0$, for simplicity.

3. Periodic Anderson model on the hypercubic lattice

We first consider the PAM on the infinite-dimensional hypercubic lattice. The bare density of states for the c band is Gaussian with the bandwidth t^*: $\rho(\omega) = \exp[-(\omega/t^*)^2]/\sqrt{\pi t^{*2}}$. In this section, we use t^* as the energy unit. The normal state properties have been discussed in detail by means of DMFT, and the phase diagram has been obtained from the divergence of the staggered susceptibility at finite temperatures.[30–33] However, the off-diagonal ordered state has not been discussed directly since it cannot easily be treated. Here, we combine DMFT

with the CTQMC method based on the Nambu formalism to discuss how the superfluid state is realized at low temperatures. In Fig. 1, we show the temperature dependence of the pair potential in the half-filled system with $U = 1$ and $V = 0.3$. At high temperatures, the pair
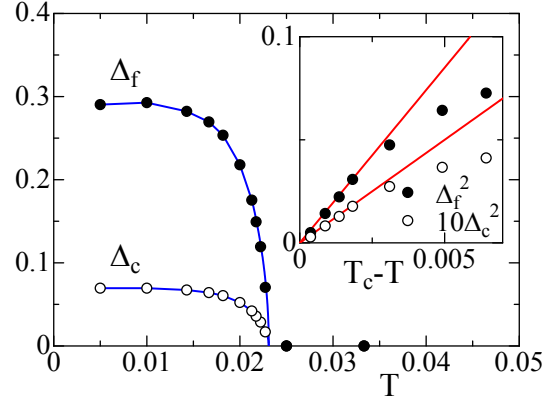

Fig. 1. (Color online) The pair potentials Δ_c and Δ_f for the superfluid state as a function of temperature T when $U = 1$ and $V = 0.3$. The inset shows the critical behavior of the pair potentials. Solid lines are guides to eyes.

potential is zero and the normal state is realized. As temperature is decreased below a critical value, the pair potentials for both bands are simultaneously induced, which implies a phase transition to the superfluid state. By examining the critical behavior $\Delta \sim |T - T_c|^\beta$ with the exponent $\beta = 1/2$, we determine the critical temperature $T_c \sim 0.023$, as shown in the inset of Fig. 1.

However, the superfluid state is not always realized at low temperatures in the PAM. By performing similar calculations for several values of the hybridization V, we find, as shown in Fig. 2, three distinct regions: $V < V_{c1}$, $V_{c1} < V < V_{c2}$ and $V_{c2} < V$. The two critical points are obtained as $V_{c1} \sim 0.26(0.18)$ and $V_{c2} \sim 0.36(0.37)$ at $T = 0.02(0.01)$. To clarify the nature of these states, we show the density of states obtained by the maximum entropy method in Fig. 3. When $V > V_{c2}$, the pair potential is zero and a charge gap appears around the Fermi level in each band. This implies that the large hybridization stabilizes the Kondo insulating state at half filling. In the intermediate region ($V_{c1} < V < V_{c2}$), the superfluid state is realized since the system has finite pair potentials and the corresponding gap in the density of states. Note that no drastic change in the density of states appears at $V = V_{c2}$, in contrast to the pair potential. A similar behavior has been discussed in the half-filled Kondo lattice model.[51] On the other hand, when $V < V_{c1}$, a finite density of states appears around the Fermi level in each band. This implies that a normal metallic state is realized.
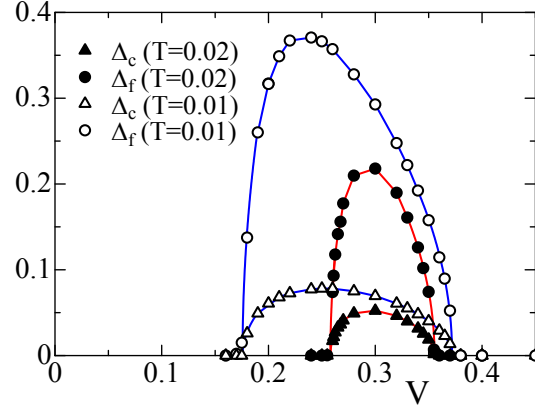
Fig. 2.   (Color online) The pair potential as a function of the hybridization V when $T = 0.01$ (open symbols) and $T = 0.02$ (solid symbols).

By performing similar calculations, we obtain the phase diagram for the half filled system with $U = 1$, as shown in Fig. 4. The normal state is realized at higher temperatures, while a different behavior appears at lower temperatures, depending on the magnitude of the hybridization. In the small V case, the system is reduced to the non-interacting c band weakly coupled to the correlated f band, which makes the critical temperature for the superfluid state rather low. Therefore, the normal metallic region shrinks as temperature is decreased, $V_{c1} \to 0$ ($T \to 0$), as shown in Fig. 4. On the other hand, we find that the other critical point V_{c2} between the superfluid state and the Kondo insulating state is slightly increased as temperature is lowered. We expect that at zero temperature, the superfluid state is realized in the small V region and a quantum phase transition occurs to the Kondo insulating state at $V_{c2}(\sim 0.38)$. This is consistent with ground-state properties for the PAM with repulsive interactions[31] and the Kondo lattice model,[42, 48] where the Kondo insulator competes with the magnetically ordered state.

Now, let us consider how the Kondo insulating state competes with the superfluid state away from half filling. In the following, we show only the pair potential Δ_f since Δ_c behaves essentially the same. In Fig. 5, we show the local particle density at each site $n(= \sum_{ai\sigma} \langle n_{i\sigma}^a \rangle / N)$ and the pair potential Δ_f when the chemical potential is varied. Here, we show only the local particle density at $T = 0.02$ in Figs. 5 (a), (b) and (c) since $n(T = 0.01)$ is almost identical. In addition, the compressibility $\kappa(= \partial n/\partial \mu)$ deduced from the numerical derivative is also shown in Fig. 5 (d). This quantity corresponds to the magnetic susceptibility in the z direction in the repulsive PAM. Therefore, a cusp singularity is naively expected at the critical point. When $V = 0.3$, the half-filled system ($\mu = 0$) is in the superfluid state at low temperatures,
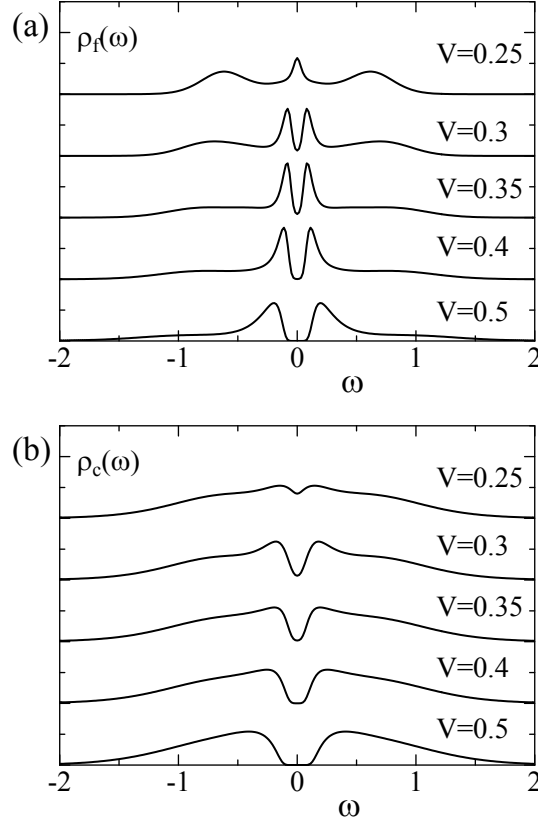
Fig. 3. (Color online) Density of states for localized and conduction bands when $V = 0.25, 0.3, 0.35, 0.4$ and 0.5 at $T = 0.02$.

as discussed above. Shifting the chemical potential away from zero, the pair potential is little affected and the local particle density varies smoothly, as shown in Fig. 5 (a). Therefore, we conclude that the superfluid state is stable against small changes in the chemical potential. Far away from half filling, the pair potential decreases and finally reaches zero. A phase transition then occurs to the normal metallic state. By contrast, a different behavior appears in the case $V = 0.35$. The pair potential initially increases as the chemical potential is shifted away from zero, has a maximum value around $\mu \sim 0.05$, and finally vanishes at the phase transition, as shown in Fig. 5 (b). The nonmonotonic behavior is even more clearly evident in the case $V = 0.4$, as shown in Fig. 5 (c). When $\mu < \mu_{c1}$, where $\mu_{c1} \sim 0.049(0.032)$ at $T = 0.02(0.01)$, the pair potential is zero and the local particle density is little changed. In fact, Fig. 5 (d) shows the strong suppression in the compressibility. This implies that an incompressible Kondo insulating state is realized at half filling, instead of the superfluid state. An increase in the chemical potential beyond μ_{c1} drives a chemical potential-induced superfluid phase transition, marked by the appearance of the pair potential and a cusp singularity
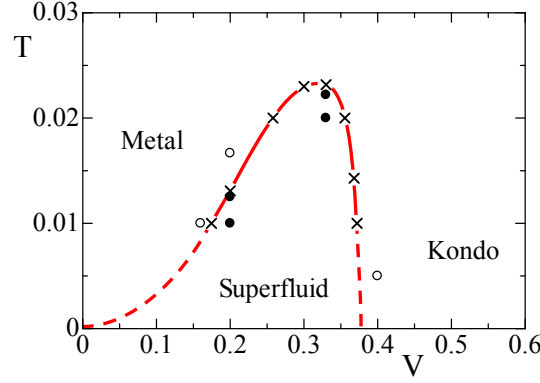
Fig. 4. (Color online) Phase diagram of the half-filled PAM with $U = 1$. Crosses are the critical points, solid (open) circles indicate the state with (without) the pair potential. The phase boundary is a guide to the eyes.
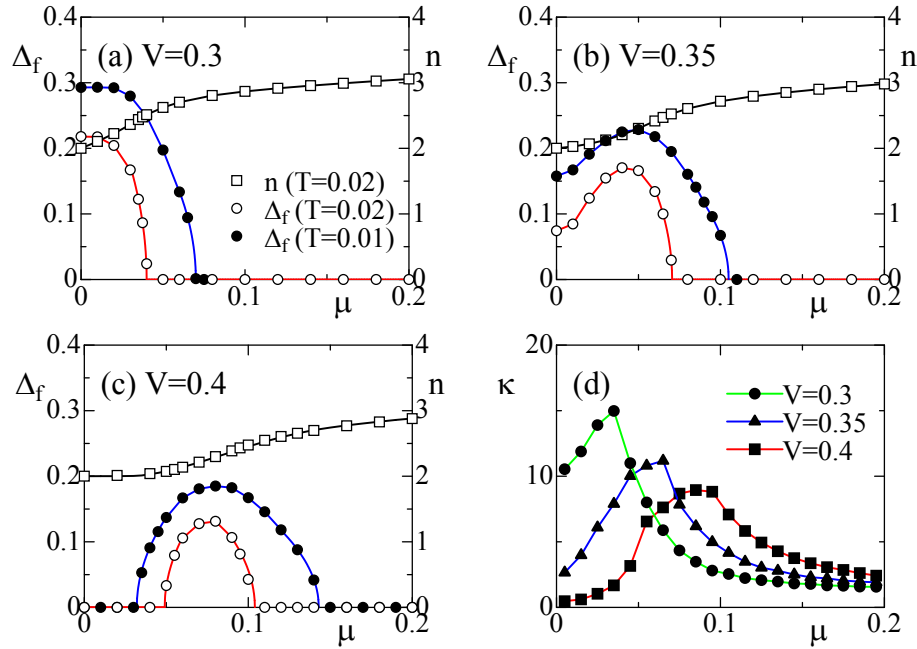

Fig. 5. (Color online) The local particle density and the pair potential for the f band as a function of the chemical potential when $V = 0.3$ (a), $V = 0.35$ (b), and $V = 0.4$ (c). (d) The compressibility of the system with $V = 0.3, 0.35$ and 0.4 at $T = 0.02$.

in the compressibility although the latter is not clearly visible in Fig. 5 (d). Further increase in μ changes the local particle density and finally drives the system to the normal metallic state at $\mu = \mu_{c2}$, where $\mu_{c2} \sim 0.10(0.14)$ at $T = 0.02(0.01)$.

By performing similar calculations for various temperatures, we obtain the phase diagram for $U = 1$ and $V = 0.4$ shown in Fig. 6. This is essentially the same as the phase diagram for
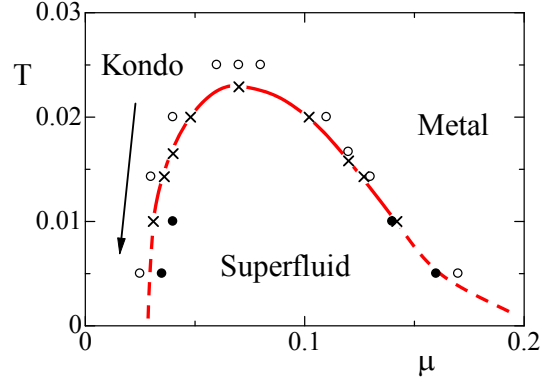
Fig. 6. (Color online) Phase diagram for the system with $U = 1$ and $V = 0.4$. Crosses are the critical points, solid (open) circles indicate the state with (without) the pair potential. The phase boundary is a guide to the eyes.

the magnetic field in the PAM with repulsive interactions.[34–36] When the system is half filled ($\mu = 0$), the Kondo insulating state is realized at low temperatures. At $T = 0.01$, two peak structures clearly appear at the edges of the hybridization gap in the density of states of the f band, as shown in Fig. 7 (a). The introduction of the chemical potential simply shifts these
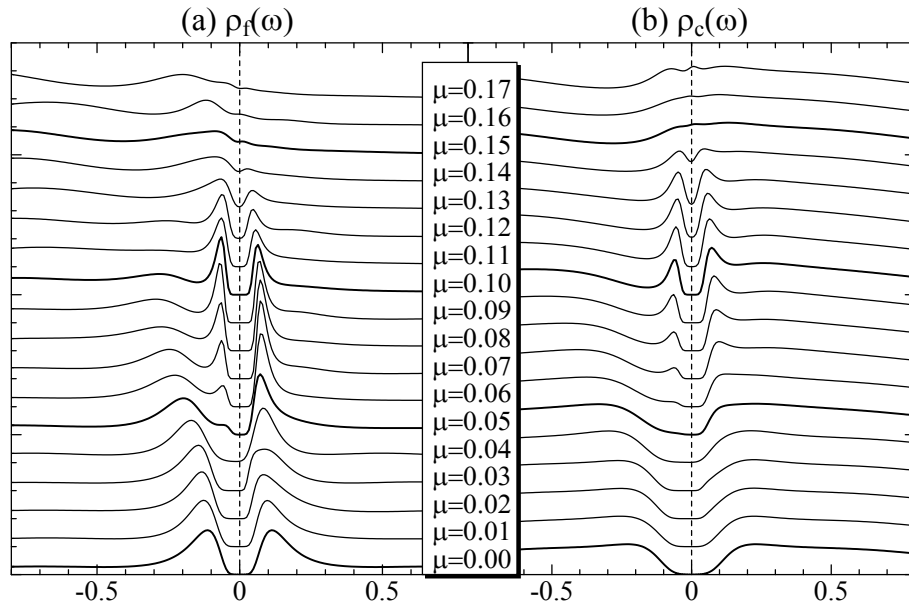

Fig. 7. Density of states for the f (a) and c (b) bands of the system with $U = 1$ and $V = 0.4$ at $T = 0.01$. The data are for the chemical potentials $\mu = 0.00, 0.01, \cdots, 0.17$ from the bottom to the top.

peaks in the case $\mu < 0.03$ since the Kondo state is incompressible. Further increase leads to

interesting behavior in the density of states. We find that around $\mu \sim 0.05$, the upper peak never approaches the Fermi level and low energy states are, instead, induced below the Fermi level between the two peaks. This implies that particles in the vicinity of the Fermi level form Cooper pairs, which yields low-energy in-gap states. The latter interpretation is consistent with the fact that the chemical potential-induced superfluid phase transition occurs at $\mu_{c1} \sim 0.032$. When the chemical potential increases beyond the critical point, the low-energy feature grows and becomes the dominant peak. It is also found that as the chemical potential is varied, the center of the gap is always located at the Fermi level, in contrast to the case with $\mu < \mu_{c1}$. On the other hand, the peak at the lower edge of the hybridization gap becomes smeared. Therefore, we conclude that a compressible superfluid state is stabilized in this region. When the system approaches $\mu_{c2}(\sim 0.14)$, the superfluid gap collapses and another phase transition occurs to the normal metallic state. A similar behavior is also found in the density of states of the c band, as shown in Fig. 7 (b). We emphasize that our calculation directly treats the low temperature superfluid state, in contrast to previous works for the PAM.[34–36] Figure 7 therefore clarifies how the chemical potential-induced phase transition yields low energy in-gap states in the density of states.

The results obtained above may have important consequences for three-dimensional optical lattice systems. In particular, one might expect quantum critical behavior in the vicinity of a certain surface in the three-dimensional optical lattice system if the confining potential is regarded as a site-dependent chemical potential. In the following section, we study the effect of the confining potential carefully to discuss the competition between the Kondo insulating state and the superfluid state in such optical lattice systems.

4.   Effect of the confining potential

We study here the effect of the confining potential in the PAM. As discussed in the previous section, we have found that the Kondo insulating state competes with the superfluid state at low temperatures. Furthermore, it has been clarified that in a certain parameter region, a shift of the chemical potential can stabilize the superfluid state. Therefore, if the confining potential is simply regarded as a site-dependent chemical potential, the Kondo insulating state and the superfluid state may be separated by a quantum critical surface in the three-dimensional optical lattice system. In this case, the critical temperature should depend on the position in the trap. However, the physics in the presence of a trap is highly nontrivial and therefore it is necessary to discuss the low temperature properties using more sophisticated tools.

To this end, we use the real-space DMFT. The method is based on the local approximation, but intersite correlations are to some extent taken into account. In fact, the real-space DMFT approach has been successfully used to discuss low temperature properties of optical lattice systems[46, 52–54)] and the interface between transition metal oxides.[55)] Here, making use of this method, we consider a three-dimensional optical lattice system. The Hamiltonian for the confining potential is defined as,

$$H_c = \sum_{ia\sigma} v(r_i) n^a_{i\sigma}, \tag{13}$$

where $v(r) = v_0(r/a)^2$, v_0 is the curvature of the confining potential, r_i is the distance between the ith site and the center of the trap, and a is the lattice constant. In this section, we fix $t = 1$ and $v_0 = 0.1$. We then treat a system with 4169 sites restricted by the condition $(r/a \leq 10)$. Using the CTQMC method as an impurity solver, we perform the real-space DMFT calculations. We obtain results for the spatial distributions of the local particle density and the pair potentials for the system with $U = 3.5$ and $\mu = 0.5$, as shown in Fig. 8. When the
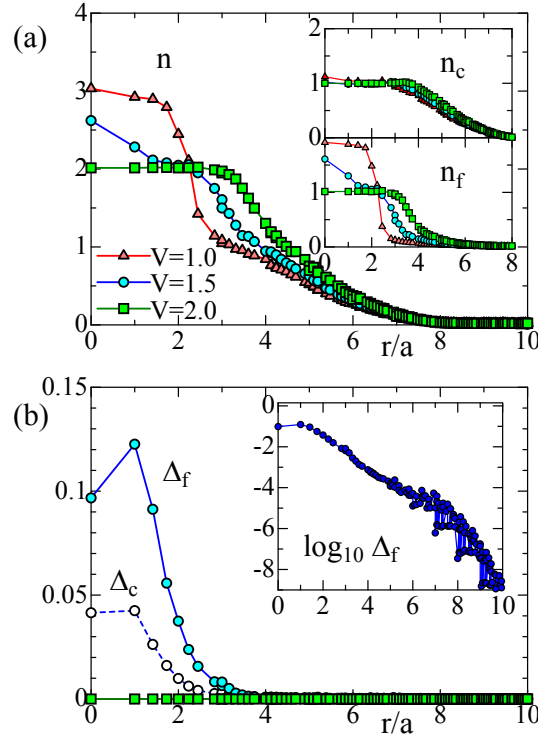

Fig. 8. (Color online) Local particle density (a) and the pair potentials (b) as a function of the distance from the center in the three-dimensional optical lattice system. Triangles, circles, and squares represent the results in the system with $V = 1.0, 1.5$ and $V = 2.0$ when $U = 3.5$ and $T = 0.033$. The inset of figure (a) shows the local particle density for the c and f bands. The pair potential is shown on a logarithmic scale in the inset of the figure (b).

hybridization is small ($V = 1.0$), the localized f particles are weakly coupled to the c band. Therefore, the f band is almost occupied in the core $r/a \lesssim \sqrt{\mu/v_0} \sim 2.2$, and empty outside the core due to the attractive interaction for the f band. By contrast, the noninteracting c particles are widely distributed due to the hopping integral between sites, as shown in the inset of Fig. 8 (a). In this case, no pair potential appears and the metallic state is realized. An increase in the hybridization affects the distribution of the f band and low-temperature properties. When $V = 1.5$, the local particle density around the center is decreased and the pair potential is induced in the system, as shown in Fig. 8. Therefore, the superfluid state is realized in the whole region with $n(r) \neq 0$ although the pair potential is tiny away from the center, as shown in the inset of Fig. 8 (b). This behavior is similar to that in the attractive Hubbard model with a confining potential.[46] Note that the rapid decay in the pair potential sets in around $r/a = 1$, in contrast to the distribution of the local particle density. This may be explained by the competition between the Kondo insulating state and the superfluid state. We find a shoulder structure around $r/a = 2$ in the local particle density, which indicates a tendency to form the Kondo insulating state in the superfluid state. This results in the rapid decay of the pair potential. Further increase in the hybridization tends to result in a plateau structure and decreases the pair potential. When $V = 2.0$, the pair potential vanishes and the plateau clearly appears at a value of $n(r)$ corresponding to half of the states occupied. Therefore, the Kondo insulating state is stabilized in the core region with $r/a \lesssim 3$.

With these calculations, we have clarified that the Kondo insulating state spatially competes with the superfluid state in an optical lattice system with confining potential. However, we could not find a critical surface between the superfluid state and the Kondo insulating state, which could naively be expected from the results of the infinite dimensional PAM. Therefore, we can say that intersite correlations play an important role and must be considered in a discussion of the low temperature properties of optical lattice systems.

Before concluding the paper, we would like to comment on correlation effects in the c band, which can be tuned by the Feshbach resonance in optical lattice systems. According to previous studies of the PAM with repulsive interactions, these interactions do not affect the low temperature properties qualitatively.[56,57] Therefore, it is expected that in the attractive case, the essence of the low temperature properties must be described by the simple PAM [eq. (1)] although phase boundaries may be slightly shifted by interactions between the c particles.

5. Summary

We have investigated the periodic Anderson model with attractive interactions on the hypercubic lattice. By combining DMFT with the CTQMC method based on the Nambu formalism, we have studied quantitatively how the superfluid state is stabilized at low temperatures. It has been found that a low-energy state characteristic of the superfluid phase appears in the hybridization gap near the critical chemical potential. We have also discussed the effect of the confining potential in the three-dimensional optical lattice by means of the real-space DMFT to clarify how the superfluid state spatially competes with the Kondo insulating state.

Acknowledgement

References

1) For a review, see Nature (London) **416** (2002) 205-246.

2) C. J. Pethick and H. Smith, *Bose-Einstein Condensation in Dilute Gases* (Cambridge University Press, Cambridge, 2002).

3) L. Pitaevskii and S. Stringari, *Bose-Einstein Condensation* (Clarendon Press, Oxford, 2003).

4) M. H. Anderson, J. R. Ensher, M. R. Matthews, C. E. Wieman, and E. A. Cornell: Science **269** (1995) 198.

5) I. Bloch and M. Greiner: *Advances in Atomic, Molecular, and Optical Physics*, edited by P. Berman and C. Lin (Academic Press, New York, 2005), Vol. 52 p. 1.

6) I. Bloch: Nature Physics **1** (2005) 23.

7) D. Jaksch and P. Zoller: Ann. Phys. (NY) **315** (2005) 52.

8) O. Morsch and M. Oberhaler: Rev. Mod. Phys. **78** (2006) 179.

9) R. Jördens, N. Strohmaier, K. Günter, H. Moritz, T. Esslinger: Nature **455** (2008) 204.

10) U. Schneider, L. Hackermüller, S. Will, Th. Best, I. Bloch, T. A. Costi, R. W. Helmes, D. Rasch, and A. Rosch: Science **322** (2008) 1520.

11) S. Jochim, M. Bartenstein, A. Altmeyer, G. Hendl, S. Riedl, C. Chin, J. Hecker Denschlag, and R. Grimm: Science **302** (2003) 2101.

12) M. W. Zwierlein, C. A. Stan, C. H. Schunck, S. M. F. Raupach, S. Gupta, Z. Hadzibabic, and W. Ketterle: Phys. Rev. Lett. **91** (2003) 250401.

13) T. Bourdel, L. Khaykovich, J. Cubizolles, J. Zhang, F. Chevy, M. Teichmann, L. Tarruell, S. J. J. M. F. Kokkelmans, and C. Salomon: Phys. Rev. Lett. **93** (2004) 050401.

14) T. B. Ottenstein, T. Lompe, M. Kohnen, A. N. Wenz, and S. Jochim: Phys. Rev. Lett. 101 (2008) 203202.

15) J. H. Huckans, J. R. Williams, E. L. Hazlett, R. W. Stites, and K. M. O'Hara: Phys. Rev. Lett. 102 (2009) 165302.

16) T. Fukuhara, S. Sugawa, Y. Takasu, and Y. Takahashi: Phys. Rev. A **79** (2009) 021601.

17) A. V. Gorshkov, M. Hermele, V. Gurarie, C. Xu, P. S. Julienne, J. Ye, P. Zoller, E. Demler, M. D. Lukin, and A. M. Rey: Nat. Phys. **6** (2010) 289.

18) M. Foss-Feig, M. Hermele, and A. M. Rey: Phys. Rev. A **81** (2010) 051603.

19) M. Foss-Feig, M. Hermele, V. Gurarie, and A. M. Rey: arXiv:1007.5083.

20) A. C. Hewson, *The Kondo Problem to Heave Fermions*, Cambridge University Press (Cambridge, 1993).

21) W. Metzner and D. Vollhardt: Phys. Rev. Lett. **62** (1989) 324.

22) E. Müller-Hartmann: Z. Phys. B **74** (1989) 507.

23) A. Georges, G. Kotliar, W. Krauth, and M. J. Rozenberg: Rev. Mod. Phys. **68** (1996) 13.

24) T. Pruschke, M. Jarrell, and J. K. Freericks: Adv. Phys. **44** (1995) 187.

25) A. N. Rubtsov, V. V. Savkin and A. I. Lichtenstein: Phys. Rev. B **72** (2005) 035122.

26) H. Shiba: Prog. Theor. Phys. **48** (1972) 2171.

27) H. Schweitzer and G. Czycholl: Z. Phys. B **79** (1990) 377; Phys. Rev. Lett. **67** (1991) 3724.

28) T. Mutou and D. Hirashima: J. Phys. Soc. Jpn. **63** (1994) 4475; J. Phys. Soc. Jpn. **64** (1995) 4799; T. Saso and M. Itoh: Phys. Rev. B **53** (1996) 6877.

29) P. S. Riseboorough: Phys. Rev. B **45** (1992) 13984; V. Dorin and P. Schlottmann: Phys. Rev. B

46 (1992) 10800;

30) M. Jarrell, H. Akhlaghpour, and Th. Pruschke: Phys. Rev. Lett. **70** (1993) 1670; M. Jarrell: Phys. Rev. B **51** (1995) 7429.

31) M. J. Rozenberg: Phys. Rev. B **52** (1995) 7369.

32) Y. Imai and N. Kawakami: Acta Phys. Pol. B **34** (2003) 779.

33) A. Koga, N. Kawakami, R. Peters, and Th. Pruschke: Phys. Rev. B **77** (2008) 045120; J. Phys. Soc. Jpn. **77** (2008) 033704.

34) K. S. D. Beach, P. A. Lee, and P. Monthoux: Phys. Rev. Lett. **92** (2004) 026401.

35) I. Milat, F. Assaad, and M. Sigrist: Eur. Phys. J. B **38** (2004) 571.

36) T. Ohashi, A. Koga, S. Suga, and N. Kawakami: Phys. Rev. B **70** (2004) 245104.

37) M. Caffarel and W. Krauth: Phys. Rev. Lett. **72** (1994) 1545.

38) H. R. Krishna-murthy, J. W. Wilkins, and K. G. Wilson: Phys. Rev. B **21** (1998) 1003.

39) R. Bulla, T. Costi, and Th. Pruschke: Rev. Mod. Phys. **80** (2008) 395.

40) P. Werner, A. Comanac, L. de'Medici, M. Troyer, and A. J. Millis: Phys. Rev. Lett. **97** (2006) 076405.

41) P. Werner and A. J. Millis: Phys. Rev. B **75** (2007) 085108.

42) P. Werner and A. J. Millis: Phys. Rev. B **74** (2006) 155107.

43) P. Werner and A. J. Millis: Phys. Rev. Lett. **99** (2007) 126405; P. Werner, E. Gull, and A. J. Millis: Phys. Rev. B **79** (2009) 115119.

44) T.-L. Dao, M. Ferrero, A. Georges, M. Capone, and O. Parcollet: Phys. Rev. Lett. **101** (2008) 236405.

45) A. Koga and P. Werner: J. Phys. Soc. Jpn. **79** (2010) 064401.

46) A. Koga, J. Bauer, P. Werner, and Th. Pruschke: arXiv:1006.4965.

47) D. J. Luitz and F. F. Assaad: Phys. Rev. B **81** (2010) 024509.

48) J. Otsuki, H. Kusunose, and Y. Kuramoto: Phys. Rev. Lett. **102** (2009) 017202.

49) F. F. Assaad and T. C. Lang: Phys. Rev. B **76** (2007) 035116; P. Werner and A. J. Millis: Phys. Rev. Lett. **99** (2007) 146404.

50) E. Gull, P. Werner, O. Parcollet and M. Troyer: Europhys. Lett. 82, (2008) 57008.

51) O. Bodensiek, Th. Pruschke, and R. Zitko: J. Phys.: Conf. Series **200** (2010) 012162.

52) R. W. Helmes, T. A. Costi, and A. Rosch: Phys. Rev. Lett. **100** (2008) 056403.

53) M. Snoek, I. Titvinidze, C. Töke, K. Byczuk, and W. Hofstetter: New. J. Phys. **10** (2008) 093008; K. Noda, A. Koga, N. Kawakami, and Th. Pruschke: Phys. Rev. A **80** (2009) 063622; Blümer and E. V. Gorelik: arXiv:1006.2716.

54) A. Koga, T. Higashiyama, K. Inaba, S. Suga, and N. Kawakami: J. Phys. Soc. Jpn. **77** (2008) 073602; Phys. Rev. A **79** (2009) 013607.

55) S. Okamoto and A. Millis: Phys. Rev. B **70** (2004) 241104.

56) T. Schork and S. Blawid: Phys. Rev. B **56** (1997) 6559.

57) R. Sato, T. Ohashi, A. Koga, and N. Kawakami: J. Phys. Soc. Jpn. **73** (2004) 1864.